Alpha and theta activity during reward anticipation are modulated by implicit expectations about sequential risk

Eszter Tóth-Fáber[1] and Andrea Kóbor[2,*]

1: Brain, Memory and Language Research Group, Institute of Cognitive Neuroscience and Psychology, HUN-REN Research Centre for Natural Sciences, *Budapest, Hungary*

2: Brain Imaging Centre, HUN-REN Research Centre for Natural Sciences, *Budapest, Hungary*

*: Corresponding author:

Andrea Kóbor

Brain Imaging Centre, HUN-REN Research Centre for Natural Sciences

Magyar tudósok körútja 2, H–1117, Budapest, Hungary

E-mail: kobor.andrea@ttk.hu

Running title: Reward anticipation in sequential risk taking

Abstract

Reward anticipation potentially guides sequential decision making, yet its underlying neural dynamics remain unclear. In this study, we investigated how risk levels and uncertainty modulate oscillatory brain activity during reward anticipation. EEG was recorded while participants (N = 44) performed a modified version of the Balloon Analogue Risk Task where balloon burst probabilities changed throughout the task, promoting uncertainty. We analyzed induced spectral power time-locked to three risk levels: early no-risk pumps, final successful pumps (preceding a cash out), and unsuccessful pumps (preceding a balloon burst). Time–frequency decomposition using Morlet wavelets revealed a parieto-occipital alpha power increase following early no-risk pumps, interpreted as disengagement from deliberative processing when anticipating sure rewards. In contrast, centroparietal alpha and frontocentral theta power decreased most prominently following final successful pumps, suggesting heightened attentional and expectancy-related processes in response to high reward potential. The results indicate that alpha and theta dynamics are sensitive to risk levels and reward expectations. These findings provide novel insights into the oscillatory mechanisms of reward anticipation in uncertain decision environments.

Keywords: alpha power, Balloon Analogue Risk Task, reward anticipation, theta power, time–frequency analysis, uncertain decision making

Introduction

Reward processing is a complex neurocognitive phenomenon that unfolds across two temporally distinct stages: reward anticipation and reward outcome (Alí Diez, Fàbrega-Camps, Parra-Tíjaro, & Marco-Pallarés, 2024; Berridge, Robinson, & Aldridge, 2009; Glazer, Kelley, Pornpattananangkul, Mittal, & Nusslock, 2018; Meyer, Marco-Pallarés, Boulinguez, & Sescousse, 2021). While extensive research has examined the neural mechanisms underlying reward outcome, the spectral EEG dynamics associated with reward anticipation remain relatively underexplored (for review, see Meyer et al., 2021). Understanding these dynamics is crucial, as reward anticipation plays a key role in guiding decision making, particularly in uncertain environments where learning from and predicting probabilistic rewards are essential (Alí Diez et al., 2024; Berridge & Robinson, 2003).

Most of our daily decisions take place under uncertain conditions, requiring us to gradually learn the probabilities of different outcomes (De Groot & Thurik, 2018; Hertwig & Erev, 2009; Knight, 1921). For example, when playing an arcade claw machine game with a limited number of coins, we make repeated decisions on whether to continue playing based on previous successes or failures. Each time we insert a coin and control the claw, we anticipate whether we will successfully grab a prize or not. If the claw has weak grip strength multiple times in a row, we might expect failure and hesitate to keep playing. Conversely, a series of successful or nearly successful grabs might encourage further attempts. This sequential decision-making process mirrors how individuals adjust expectations and risk-taking behavior in uncertain situations. Yet, it remains unclear whether risk and uncertainty shapes anticipatory neural activity at the time-frequency level. To bridge this research gap, we investigate how these factors influence EEG spectral dynamics during reward anticipation after the decision has been made in a task simulating real-life risk taking.

To this end, we use a modified version of the Balloon Analogue Risk Task (BART), a well-established paradigm for studying naturalistic risk-taking behavior (De Groot, 2020; Helfinstein et al., 2014; Lejuez et al., 2002; Schonberg, Fox, & Poldrack, 2011). In this task, participants make sequential decisions to inflate a virtual balloon, thereby increasing the potential rewards while also increasing the a priori unknown probability of the balloon bursting, which would result in the loss of accumulated earnings. Previous event-related brain potential (ERP) studies have explored reward processing within this paradigm, focusing primarily on the outcome stage (e.g., Gu, Zhang, Luo, Wang, & Broster, 2018; Kardos et al., 2016; Kiat, Straley, & Cheadle, 2016; Kóbor et al., 2015; Petropoulos Petalas, Bos, Hendriks Vettehen, & van Schie, 2020; Xu, 2021). Some of these studies have demonstrated progressive expectation formation about the reward structure of the task (Kardos et al., 2016; Kiat et al., 2016; Petropoulos Petalas et al., 2020). However, the investigation of reward expectation and anticipation was conducted indirectly through the analysis of outcome-related processing at the various steps of the balloon inflation process using stimulus-locked ERPs. Consequently, the EEG dynamics related to each pump during balloon inflation, while awaiting and anticipating the outcome (inflated balloon or balloon burst), remain to be elucidated. The latter approach, which is also employed in this study, has the potential to directly reveal whether reward expectation and anticipation undergo changes over the course of the task.

Reward expectation and anticipation can change dynamically as the underlying task regularities shift, influencing perceived levels of risk and uncertainty. Earlier studies using the BART have shown that different burst probability functions can be learned, leading to behavioral adaptations (Bonini, Grecucci, Nicolè, & Savadori, 2018; Kóbor et al., 2021; Kóbor et al., 2023; Koscielniak, Rydzewska, & Sedek, 2016; Smith, Ebert, & Broman-Fulks, 2016; Young & McCoy, 2019). Therefore, the present study incorporates a three-phase manipulation – baseline, lucky, and unlucky phases – to systematically vary levels of uncertainty. The lucky

phase features a reduced burst probability, making risk taking more favorable, while the unlucky phase increases burst probability, creating a high-risk environment. We have already shown that different levels of uncertainty due to this manipulation impact how individuals learn from rewards, as revealed by computational modeling and behavioral indices (Bán, Tóth-Fáber, Lages, & Kóbor, 2024). Specifically, heightened sensitivity to rewards relative to losses was associated with heightened risk-taking behavior across all phases. This heightened sensitivity was found to be inversely correlated with task performance during periods of high uncertainty. In this study, we build upon this work by examining the spectral EEG components associated with reward anticipation, which underpin the processing of varying levels of uncertainty throughout the balloon inflation process.

EEG time-frequency measures provide several advantages over traditional ERP analyses. Unlike ERPs, which primarily reflect phase-locked activity, time-frequency analyses can also capture non-phase-locked oscillatory dynamics, providing a richer representation of neural activity (Alí Diez et al., 2024; Bastiaansen, Mazaheri, & Jensen, 2012; Cohen, 2014; Glazer et al., 2018; Li, Baker, Warren, & Li, 2016; Makeig et al., 2002; Tallon-Baudry & Bertrand, 1999). These measures can allow us to investigate the fine-grained temporal dynamics of anticipatory neural activity. So far, with time-frequency analysis, research on sequential risk taking using variants of the BART has targeted only the processing of reward outcomes. In the outcome stage, midfrontal theta activity has been shown to vary depending on outcome type (Edgar et al., 2024), personality traits related to risk taking (Edgar et al., 2024; Qianlan, Shou, Tianya, Wei, & Liu, 2025), and gain/loss framing (Tao et al., 2023). To our knowledge, no studies have investigated time-frequency dynamics during reward anticipation in this task.

In the context of reward anticipation, characteristics of EEG time-frequency components have been predominantly examined within paradigms that diverge from the BART, including monetary incentive delay and time-estimation tasks with cue-target-outcome

structures. In this earlier research, parieto-occipital alpha suppression has been found to reflect increased attention allocation and disinhibition of sensory cortices in preparation for outcome processing (Bastiaansen, Böcker, & Brunia, 2002; Bastiaansen & Brunia, 2001; Gómez, Vaquero, López-Mendoza, González-Rosa, & Vázquez-Marrufo, 2004; Pornpattananangkul & Nusslock, 2016; van den Berg, Krebs, Lorist, & Woldorff, 2014; Zhang et al., 2023). This suppression is typically greater before rewarding than nonrewarding outcomes as well as before high than low magnitude outcomes, suggesting its role in facilitating adaptive behavior. Additionally, anterior beta activity has also been associated with reward anticipation, often increasing before higher potential rewards, indicative of incentive-motivational processes (Apitz & Bunzeck, 2014; Bunzeck, Guitart-Masip, Dolan, & Düzel, 2011; Reinhart & Woodman, 2014; Xiao et al., 2024). However, findings regarding frontocentral theta activity have remained mixed. Some EEG studies report an increase in theta activity before (higher) potential rewards (Alí Diez et al., 2024; Fryer et al., 2021; Reinhart & Woodman, 2014; Zhang et al., 2023), whereas others find a decrease (Bunzeck et al., 2011; Doñamayor, Schoenfeld, & Münte, 2012) or no change (Lopez-Gamundi, Mas-Herrero, & Marco-Pallares, 2024) associated with increasing reward probability. The general reduction of EEG power during expectancy periods has also been noted in a nonrewarded cue-target paradigm, further emphasizing the complexity of anticipatory neural dynamics (Gómez et al., 2004).

Building on this background, we examine how different levels of risk and uncertainty influence EEG spectral activity during reward anticipation in the BART. We leverage previously established experimental contrasts (Kardos et al., 2016) that capture reward expectation evolving throughout the balloon inflation process. These contrasts define the key risk steps that we analyze in this study (see Figure 1). The first step is the early no-risk pump, where the anticipation of a sure reward (inflated balloon) is associated with this pump. The second step is the final pump prior to cashing out. Due to the success of this final pump, a

reward occurs eventually. The third step is the pump leading to a balloon burst. The second and third steps are located at the end of the balloon trial, and subsequent to both of these steps, either a balloon burst or a reward may be anticipated. Critically, the outcome remains unpredictable until the moment it occurs. According to the findings of ERP and fMRI studies conducted previously, there is an indication that brain responses might vary prior to cashing out as opposed to pumping towards a balloon burst (i.e., reward positivity and P3 amplitudes, cognitive control networks, see Helfinstein et al., 2014; Kardos et al., 2016). Consequently, the question remains open regarding whether and, if so, how anticipation differs between the final successful and unsuccessful pumps. In addition to these risk levels, we examine the effect of uncertainty introduced by the three-phase task structure (baseline, lucky, unlucky). Note that participants were not informed about burst probabilities, the changes in these probabilities across task phases (i.e., uncertainty), and the zero probability of balloon burst after the initial two pumps.

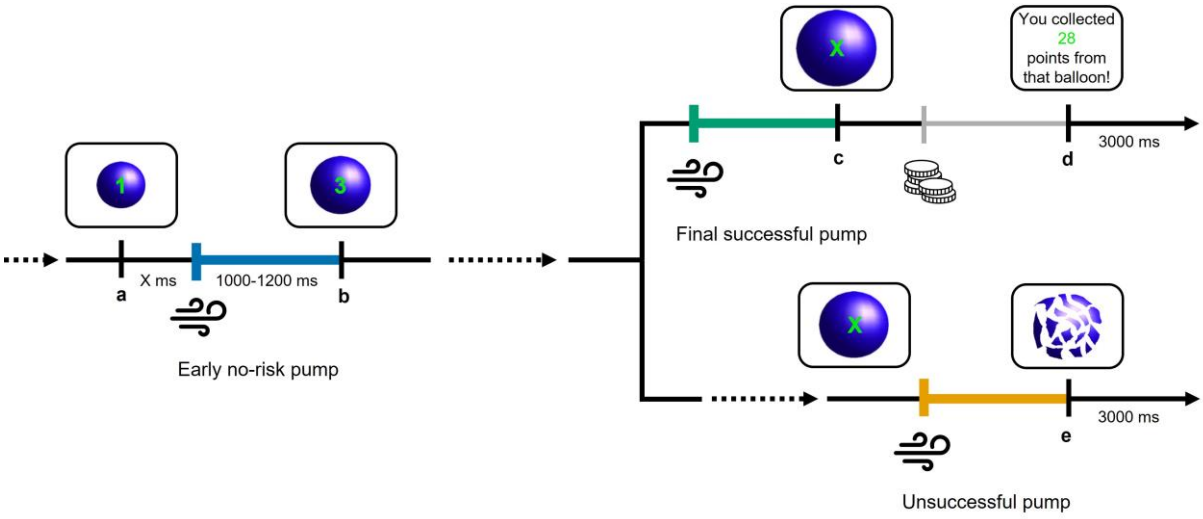

Figure 1. Schematic illustration of the trial structure and the key risk steps in the BART. Each balloon trial started with the presentation of a zero-value balloon (not indicated in this figure). Lowercase capital letters (a, b, c, d, e) denote the onsets of balloon presentation after the first (a), second (b), and further (c) pumps, and the onsets of feedback presentation at the end of the balloon trial (d = cash-out screen for successful ballon trials, e = balloon burst for unsuccessful balloon trials). The blow icons represent the onset of the pump response, relative to which the EEG segments were synchronized in time. The coins icon represents the onset of the cash-out response, by which participants could collect the accumulated score from the current balloon and end the balloon trial. The score accumulated in the current balloon trial was presented in the middle of the balloon during the task. Participants had no time limit ("X ms") to respond to the current balloon, i.e., to pump the balloon further or to cash out. After each successful pump, one point more was added to the accumulated score (1, 3, 6, 10, 15, etc., presented as the accumulated score). Each response was followed by the inflated balloon stimulus (reward) or the

end-of-trial feedback stimulus (cash-out screen or burst stimulus) after a random delay of 1000-1200 ms. This delay period was considered as the reward anticipation stage, where EEG spectral dynamics were analyzed by time-frequency analysis. Note that the current balloon was presented on the screen throughout the response and delay periods (i.e., until the onset of the next balloon or that of the feedback). The blue-, green-, and yellow-colored, thick sections of the timeline denote the reward anticipation stages. The blue section is the anticipatory stage after the early no-risk (second) pump, the green section is the anticipatory stage after the final successful pump before cashing out, and the yellow section is the anticipatory stage after the unsuccessful pump leading to a balloon burst. The occurrence of the final successful pump, as well as the unsuccessful pump, is possible at any subsequent time point (denoted by dashed arrow lines) after the early no-risk pump. Therefore, the exact value of the balloon is not given for these risk steps (indicated by green "X"). The anticipatory stage after the cash-out response (grey-colored, thin section) was not analyzed. For more details on the task structure and the expectedness of the reward, see the main text. This illustration has been adapted from the figure published by Kardos et al. (2016).

Regarding the risk levels, we hypothesize that alpha suppression will become more pronounced as risk increases throughout the balloon inflation process, with the largest suppression following both successful and unsuccessful pumps at the final inflation step. At the early no-risk inflation step, alpha power may instead increase, reflecting neural inhibition necessary for continuing the inflation process without deliberation (Klimesch, 2012). Beta power is expected to be modulated by outcome probability, increasing when reward probability is higher at the early no-risk step. Furthermore, theta power is assumed to decrease when the reward is more probable (Bunzeck et al., 2011; Doñamayor et al., 2012), leading to theta suppression at the early no-risk inflation step and relatively increased theta at the final step, after both successful and unsuccessful pumps. Beyond reward probability, the magnitude of the potential reward could also induce theta enhancement at the final inflation steps relative to the early no-risk step (Zhang et al., 2023). Alpha, beta, and theta power may differentiate between successful and unsuccessful balloon inflations; however, this remains an exploratory question (Helfinstein et al., 2014; Kardos et al., 2016).

Regarding uncertainty, we predict that alpha suppression will be strongest in the uncertain unlucky phase, while beta power will be higher in phases with more probable rewards (lucky and baseline phases). To adequately respond to the heightened incentive value of the reward and the risk of potential loss during the lucky and unlucky phases, generally enhanced

top-down control may be necessary. Hence, theta power may increase in these phases relative to the baseline phase (Zhang et al., 2023). In particular, enhanced top-down control could be required due to heightened performance monitoring demands in the unlucky phase and greater effort investment in the lucky phase, where participants may persist longer to achieve a larger reward (Lopez-Gamundi et al., 2024). Finally, we hypothesize an interaction between uncertainty and increasing risk, with the above-mentioned time-frequency modulations across risk levels being most pronounced in the high-uncertainty (unlucky) phase. Through these analyses, we aim to provide novel insights into the spectral dynamics of reward anticipation under conditions of varying risk and uncertainty, advancing our understanding of neurocognitive mechanisms supporting sequential decision making.

Materials and methods

Participants

Fifty young adults took part in the experiment. They were recruited from university courses and were randomly assigned to one of the two order conditions (about the order, see Task section). All participants had normal or corrected-to-normal vision, reported no history of psychiatric or neurological disorders, and were not taking any psychoactive medication at the time of participation. Handedness was assessed using the revised version of the Edinburgh Handedness Inventory (Dragovic, 2004a, 2004b; Oldfield, 1971). The mean laterality quotient was 75.71 (SD = 40.68; −100 means complete left-handedness, 100 means complete right-handedness). During the EEG analyses, six participants were excluded due to excessive artifacts: For them, the mean ratio of the removed EEG segments was greater than 25% (for details, see EEG recording and analyses section). Hence, the final sample consisted of 44 participants (M_{age} = 21.23 years, SD_{age} = 2.52 years, 8 males, 36 females).

Prior to enrollment, all participants provided written informed consent. The study received ethical approval from the United Ethical Review Committee for Research in Psychology (EPKEB) in Hungary and was conducted in accordance with the principles of the Declaration of Helsinki. In exchange for their participation, students received course credit and a supermarket voucher. Although the participants were informed that the value of the voucher would depend on their task performance (ranging from 1000 to 2000 HUF, approximately €2.5–€5), all received a voucher worth 2000 HUF upon completion of the experiment.

Task

A modified version of the Balloon Analogue Risk Task (BART; Alí Diez et al., 2024; Bán et al., 2024; Fein & Chang, 2008; Kóbor et al., 2015; Kóbor et al., 2023; Lejuez et al., 2002) was employed in the present study. During the task, participants were instructed to collect as many points as possible by inflating virtual balloons on the screen, one at a time. They were required to repeatedly decide whether to continue inflating a balloon or to stop and collect their accumulated score.

Each successful pump increased both the balloon's size and the potential reward, while simultaneously raising the probability of the balloon bursting. Participants were instructed to use two designated response keys to indicate their decision either to pump the balloon further or to terminate the trial and collect the accumulated score. Each inflation could result in one of two outcomes: either the balloon successfully inflated and the score increased, or the balloon burst, resulting in the loss of the trial's accumulated score. If participants decided to stop inflating the balloon, the score collected during that trial were transferred to a virtual permanent bank. Bursting a balloon did not affect the score stored in the permanent bank.

Throughout the task, the current trial's accumulated score was displayed within the balloon, while the permanent bank score, the score collected in the previous trial, and the

response options for pumping or cashing out were continuously visible on the screen. A balloon burst was visually indicated by a fragmented balloon stimulus, whereas cash-out trials were followed by a feedback screen displaying the score collected on that balloon trial. The duration in which a response (i.e., pump or cash out) could be initiated was unrestricted. Each response was followed by the inflated balloon stimulus (reward) or the end-of-trial feedback stimulus (cash-out screen or burst stimulus) after a random delay of 1000-1200 ms. Feedback for both cash-out and burst trials were presented for 3000 ms (Figure 1).

The task was structurally divided into three phases, each corresponding to different balloon burst probabilities. The baseline phase featured an intermediate probability of bursting. This was followed by either an increase (unlucky phase) or a decrease (lucky phase) in burst probability. All participants completed the baseline phase first. Subsequently, half were assigned to complete the lucky phase followed by the unlucky phase (Lucky-first order), while the remaining participants completed the unlucky phase first and concluded with the lucky phase (Unlucky-first order) (see also Bán et al., 2024).

In all phases, balloon bursts were disabled for the first and second pumps. In the baseline phase, the burst probability began at 1/18 on the third pump and increased gradually (1/17 on the fourth pump, 1/16 on the fifth, etc.), reaching a certainty of bursting (probability = 1) on the 20th pump. In the lucky phase, the burst probability followed a less steep trajectory (1/28 on the third pump, 1/27 on the fourth pump, 1/26 on the fifth, etc.) but burst probability was set to 1 on the 20th pump. This design was chosen to maintain a manageable average trial duration. In contrast, the unlucky phase was characterized by a steeper increase in burst probability (1/8 on the third pump, 1/7 on the fourth pump, 1/6 for the fifth, etc.), with the maximum burst probability reached on the 10th pump. (For more details, see Figure 2 in Bán et al. (2024) and Tables S2-S4 in the Supplementary Methods of Kóbor et al. (2023).) Participants were naïve regarding the burst probabilities in the experiment, including the zero probability of balloon

burst in the first two inflation opportunities. Participants were also unaware that burst probabilities would change during the experiment, and the beginning of a new phase was not signaled to them.

Each phase consisted of 90 balloon trials, out of which participants could freely decide whether they inflate the balloon or collect their accumulated score in 80 trials. In 10 trials of each phase, participants were instructed to inflate the balloon to a predetermined number of pumps or until it burst. These forced-choice trials were incorporated to provide guidance regarding the optimal number of pumps in each phase. To minimize inter-individual variability, the position of these trials was fixed and identical across all participants.

The task was implemented using Presentation software (Version 21.1; Neurobehavioral Systems, Inc., Berkeley, CA), and participants' responses were recorded via a Cedrus RB-540 response device (Cedrus Corporation, San Pedro, CA).

Procedure

Participants completed two experimental sessions. The first session involved a series of well-established neuropsychological assessments targeting executive functions, aimed at confirming that all participants performed within the neurotypical range. This session lasted approximately one hour. The second session consisted of the BART, which included both a practice and a test session. During practice, participants completed six forced-choice trials to ensure a standardized initial experience with the task. The test session consisted of 270 balloon trials (3*90) in total. To reduce fatigue, brief breaks were incorporated every 20–25 trials, with a longer break scheduled at the midpoint of the task. Continuous EEG data were recorded throughout the session. Upon completion of the BART, participants took part in a brief verbal interview, during which they were asked about their strategies and whether they had noticed

any changes in burst probabilities or differences across the task phases. The second session lasted approximately 2 to 2.5 hours, including the application and removal of the electrode cap.

Verbal interviews were recorded using a portable audio recording device (OLYMPUS WS-852). The recordings were later evaluated by an independent rater who was blind to both the research hypotheses and the experimental conditions. A bottom-up, data-driven approach was employed for the initial categorization: Participants were grouped based on the similarity of the patterns they reported noticing during the task. These groups were then categorized according to whether participants had detected the full extent of the phase-wise experimental manipulation, only partial aspects of it, or no regularities at all. Following this initial grouping, the rater was debriefed about the nature of the experimental manipulation to inform final categorization. Among the 44 participants in the final sample, 19 (43.2%) reported noticing changes consistent with the structure of the task phases, 16 (36.4%) noticed some phase-related changes without fully grasping the manipulation, and 9 (20.5%) did not report noticing any changes. Nevertheless, beyond the phase-wise changes, the participants were unable to report the burst probability functions; therefore, the deep structure of the task remained implicit.

EEG recording and analyses

The continuous EEG activity was recorded in an electrically shielded, acoustically attenuated, and dimly lit room using the actiCAP slim/snap active electrode system with BrainAmp Standard amplifier and BrainVision Recorder software (Version 1.2; BrainProducts GmbH, Gilching, Germany). EEG signals were acquired from 64 Ag/AgCl electrodes with integrated active circuits, mounted in an elastic cap and positioned according to the 10% equidistant system. The FCz electrode served as the reference, while Fpz was used as the ground. The sampling rate was 1000 Hz. Electrode impedance was maintained below 10 kΩ throughout recording.

Offline EEG processing was conducted using BrainVision Analyzer software (Version 2.2.2; BrainProducts GmbH). First, the continuous EEG data were visually inspected for major artifacts: When necessary, noisy electrodes were corrected via spherical spline interpolation, with a maximum of two interpolated electrodes per participant (M = 0.23, SD = 0.47). Second, ocular and cardiac artifacts were removed using independent component analysis (ICA; Delorme, Sejnowski, & Makeig, 2007). Between two and four components per participant were rejected (M = 2.72, SD = 0.54), after which the channel-based EEG data were recomposed. Third, the data were band-pass filtered between 0.03–30 Hz (48 dB/oct) and notch filtered at 50 Hz to remove additional electrical noise. Fourth, the data were re-referenced to the average of all electrodes, including FCz, which had served as the online reference. The FCz was then reused in the subsequent analyses. Finally, the continuous, preprocessed EEG signal was segmented according to the criteria outlined below.

Based on the key risk steps and the manipulation of burst probability across the phases, three "outcome types" were defined for EEG segmentation, each analyzed within the baseline, lucky, and unlucky phases of the task (see Figure 1). It should be noted that outcome types correspond to the risk levels (risk steps); hereafter, these terms are used interchangeably. The *early no-risk pump* was defined as the second pump of each balloon trial, during which a balloon burst was experimentally disabled. These pumps were associated with the anticipation of a guaranteed reward, as each pump was certain to result in the inflation of the balloon and an increase in the temporary score. The *final successful pump* referred to the last pump initiated before the participant chose to cash out. The *unsuccessful pump* was defined as the pump immediately preceding a balloon burst, resulting in the loss of the accumulated score. At these points in the balloon trial, the outcome remained uncertain—either a balloon burst or a reward could occur. Therefore, it can be posited that these pumps were associated with the anticipation of both outcomes.

Each response in the task was followed by a random delay of 1000-1200 ms before presenting its result (i.e., reward/inflated balloon, cash-out screen, or balloon burst, see Figure 1). EEG segments were time-locked to the pump responses that preceded the three outcome types of interest: early no-risk pumps (second pumps, when burst was disabled), final successful pumps (the last pumps before a cash out), and unsuccessful pumps (pumps that triggered a balloon burst). For each of these outcome types, segments were extracted from −200 ms to 1200 ms relative to response onset. These outcome types were extracted separately for each phase of the task (baseline, lucky, and unlucky), resulting in altogether nine experimental conditions. This segmentation framework allowed for the analysis of uncertainty- and outcome-specific neural processes underlying different forms of reward anticipation. Note that, although outcome types have been identified, they should not be confused with the potential stimulus-locked analysis of actual response outcomes.

Following segmentation, to remove remaining artifacts after ICA corrections, an automatic artifact rejection algorithm implemented in the BrainVision Analyzer software rejected segments where the activity exceeded ± 100 μV at any of the electrode sites. Across the three phases, the mean numbers of the retained (artifact-free) segments were 74.40 (*SD* = 4.27) for the early no-risk pumps, 33.28 (*SD* = 8.19) for the unsuccessful pumps, and 41.05 (*SD* = 6.81) for the final successful pumps. The mean proportion of the removed segments was 6.29% (*SD* = 5.18%) for the early no-risk pumps, 5.35% (*SD* = 5.71%) for the unsuccessful pumps, and 4.43% (*SD* = 4.08%) for the final successful pumps.

Time–frequency decomposition of the retained EEG segments was conducted using a complex Morlet wavelet transform with a Morlet parameter of 5. Frequencies ranged from 1 to 30 Hz, sampled in 30 logarithmically spaced steps. Instantaneous amplitude (Gabor normalization) was used for wavelet normalization, and the resulting spectral power was extracted as real values in units of μV^2 (Cohen, 2014). Only artifact-free segments were

included, which were baseline-corrected using the –200 to 0 ms interval preceding pump onset. For each participant, the total power was quantified as the average value of time-frequency power across single segments, while the evoked power was calculated directly from the time-frequency decomposition of the averaged segments. Induced power was determined by subtracting the evoked power from the total power (Cohen, 2014; Li et al., 2016; Tallon-Baudry & Bertrand, 1999). Importantly, only induced power was analyzed in this study. Grand averages of the induced power across participants were created separately for each combination of outcome and phase (i.e., the nine experimental conditions).

We considered whether the frequency ranges referred to in the Introduction (alpha, beta, and theta) would vary as a function of the experimental manipulations. We took into account both manipulations – risk levels and task phases – to the same degree. We determined the relevant electrodes and time windows to analyze based on the visual inspection of the grand average time-frequency plots (see Figures 3-4). An increase in alpha power was evident between 600 ms and 1000 ms in the parieto-occipital region for the early no-risk pumps (Figure 3A). Thus, we exported the spectral power from 8.26 Hz to 11.74 Hz for alpha in this time window; then, created a region of interest consisting of the O1, O2, Oz and POz electrodes for its analysis (i.e., calculated the mean of spectral power measured at these electrodes). For the final successful pumps, a decrease in both alpha and theta power was noticeable between 200 ms and 1000 ms following response onset over the centroparietal (Figure 3B) and frontocentral electrodes (Figure 4), respectively. Hence, mean spectral power was extracted from 8.26 Hz to 11.74 Hz for alpha and from 4.09 Hz to 7.34 Hz for theta over the Cz electrode in this time window. Regarding the beta frequency range, no modulations were evident either between the outcome types or the phases. Nevertheless, guided by theoretical considerations, mean spectral power was exported from 16.69 Hz to 23.73 Hz between 500 ms and 1000 ms over the left

centroparietal electrodes (C3, C5, CP3 CP5 contributing to a region of interest) identified via scalp topographies that were similar across the conditions.

Statistical analysis

To analyze basic behavioral data and mean induced power, mixed-design and repeated-measures analyses of variance (ANOVAs), respectively, were conducted. The factors involved in each analysis are specified below. The Greenhouse-Geisser epsilon correction (Greenhouse & Geisser, 1959) was used when necessary, i.e., when sphericity was violated as indicated by the significance of the Mauchly's sphericity test. Original *df* values and corrected *p* values (if applicable) are reported together with partial eta-squared (η^2_p) as the measure of effect size. Pairwise comparisons were performed using LSD (Least Significant Difference) tests. It should be noted that this paper does not offer a detailed analysis of behavioral data; for that analysis, please refer to the work of Bán et al. (2024).

Results

Behavioral results

The purpose of this analysis was to evaluate whether pumping behavior changed across the experimental phases differing in uncertainty and to check the potential effect of order manipulation (i.e., the assignment of participants to Lucky-first or Unlucky-first order). We calculated each participants' adjusted score (i.e., the mean number of pumps on unexploded balloons; Lejuez et al., 2002; Schmitz, Manske, Preckel, & Wilhelm, 2016) and their points collected in each phase. On both dependent variables separately, a mixed-design ANOVA was conducted with Order (Lucky-first vs. Unlucky-first) as a between-subjects factor and Phase (baseline vs. lucky vs. unlucky) as a within-subject factor.

Considering the adjusted score, the main effect of Order showed no differences between the two Orders ($F(1, 42) = 0.02$, $p = .89$, $\eta^2_p < .001$), while the main effect of Phase revealed that the adjusted score differed in the three phases of the task ($F(2, 84) = 235.04$, $p < .001$, $\eta^2_p = .85$). Post-hoc analysis showed that the adjusted score was the highest in the lucky phase ($M = 10.45$), slightly lower in the baseline phase ($M = 9.07$) and the lowest in the unlucky phase ($M = 4.59$), as expected (all *p*s < .001). The Order * Phase interaction was not significant ($F(2, 84) = 0.45$, $p = .59$, $\eta^2_p = .01$).

Considering the points collected, the main effect of Order revealed comparable performance in the two Orders ($F(1, 42) = 0.001$, $p = .97$, $\eta^2_p < .001$), but the main effect of Phase showed that the points collected differed in the three phases ($F(2, 84) = 194.73$, $p < .001$, $\eta^2_p = .82$). Post-hoc analysis showed that participants achieved the highest score in the lucky phase ($M = 3347.55$), followed by the baseline phase ($M = 2075.07$), with the lowest scores observed in the unlucky phase ($M = 494.30$, all *p*s < .001). The Order * Phase interaction was not significant ($F(2, 84) = 0.09$, $p = .83$, $\eta^2_p = .002$).

These behavioral results as well as our previous work on learning rates (Bán et al., 2024) indicate that the order manipulation had no effect on task performance. Therefore, the Order factor was not included in the time-frequency analyses.

Time-frequency results

To analyze how reward anticipation evolved throughout the balloon inflation process in each phase, repeated-measures ANOVAs were conducted on the mean induced power extracted for each frequency range. The ANOVA contained Outcome (early no-risk pump vs. final successful pump vs. unsuccessful pump) and Phase (baseline vs. lucky vs. unlucky) as within-subject factors.

First, the increase of alpha power in the parieto-occipital region was analyzed. The main effect of Outcome ($F(2, 86) = 7.69$, $p < .001$, $\eta^2_p = .15$) showed a significant difference in oscillatory activity between the outcome types (Figure 2B and Figure 3A). Post-hoc analysis revealed that the increase in alpha power was most pronounced after an early no-risk pump ($M = 3.95$ μV², all *p*s < .03), while it was comparable between unsuccessful and final successful pumps ($M = 2.07$ μV² vs. $M = 0.37$ μV², $p = .07$). The main effect of Phase ($F(2, 86) = 0.35$, $p = .66$, $\eta^2_p = .008$) and the Phase * Outcome interaction ($F(4, 172) = 1.06$, $p = .37$, $\eta^2_p = .02$) were not significant.

Second, an identical ANOVA was run for the decrease of alpha power over the centroparietal region. The main effect of Outcome ($F(2, 86) = 15.45$, $p < .001$, $\eta^2_p = .26$) revealed that oscillatory activity significantly differed between the outcome types (Figure 2A and Figure 3B). Post-hoc analysis showed that the decrease in alpha power was most prominent after a final successful pump ($M = -0.92$ μV², all *p*s < .001), but alpha power did not differ after an unsuccessful pump relative to an early no-risk pump ($M = -0.03$ μV² vs. $M = 0.04$ μV², $p = .69$). The main effect of Phase ($F(2, 86) = 1.11$, $p = .34$, $\eta^2_p = .03$) and the Phase * Outcome interaction ($F(4, 172) = 1.16$, $p = .33$, $\eta^2_p = .03$) were not significant.

Third, an identical ANOVA was conducted for the theta decrease over the frontocentral region. The main effect of Outcome ($F(2, 86) = 17.26$, $p < .001$, $\eta^2_p = .29$) revealed that oscillatory activity differed significantly between the outcome types. Post-hoc analysis showed a gradual change in theta power, with the most prominent decrease occurring after the final successful pump ($M = -1.42$ μV²), followed by the unsuccessful pump ($M = -0.97$ μV²), and then the early no-risk pump ($M = -0.50$ μV², all *p*s ≤ .002, Figure 2C and Figure 4). Although the main effect of Phase ($F(2, 86) = 1.79$, $p = .18$, $\eta^2_p = .04$) showed comparable oscillatory activity between the three phases, the significant Phase * Outcome interaction ($F(4, 172) = 3.44$, $p = .02$, $\eta^2_p = .07$, Figure 2D and Figure 4) revealed differences. Post-hoc analysis showed

that the differences between the outcome types were most prominent in the lucky phase, where all pairwise comparisons were significant (final successful pump: M = -1.88 μV², unsuccessful pump: M = -1.03 μV², early no-risk pump: M = -0.34 μV², all ps ≤ .003). In the baseline phase, theta power was more decreased after a final successful pump than after an early no-risk pump (M = -1.09 μV² vs. M = -0.53 μV², p = .009), while other comparisons did not reach significance (all ps > .06). Similar results were shown in the unlucky phase, with a significant difference between the final successful pump and the early no-risk pump (M = -1.28 μV² vs. M = -0.63 μV², p = .002) and no other differences (all ps > .13).

Fourth, an identical ANOVA was run for the beta power over the left centroparietal region. Neither the main effect of Outcome ($F(2, 86) = 1.72$, $p = .19$, $\eta^2_p = .04$), nor the main effect of Phase ($F(2, 86) = 2.65$, $p = .08$, $\eta^2_p = .06$), nor the Phase * Outcome interaction ($F(4, 172) = 0.27$, $p = .90$, $\eta^2_p = .006$) were significant.

To sum up the statistical findings, after the early no risk-pumps, a prominent increase in parieto-occipital alpha power was found. In addition, a pronounced decrease in centroparietal alpha power after the final successful pumps was also revealed. Over the frontocentral region, a graded pattern of theta suppression was detectable, most pronounced after the final successful pumps, especially during the lucky phase.

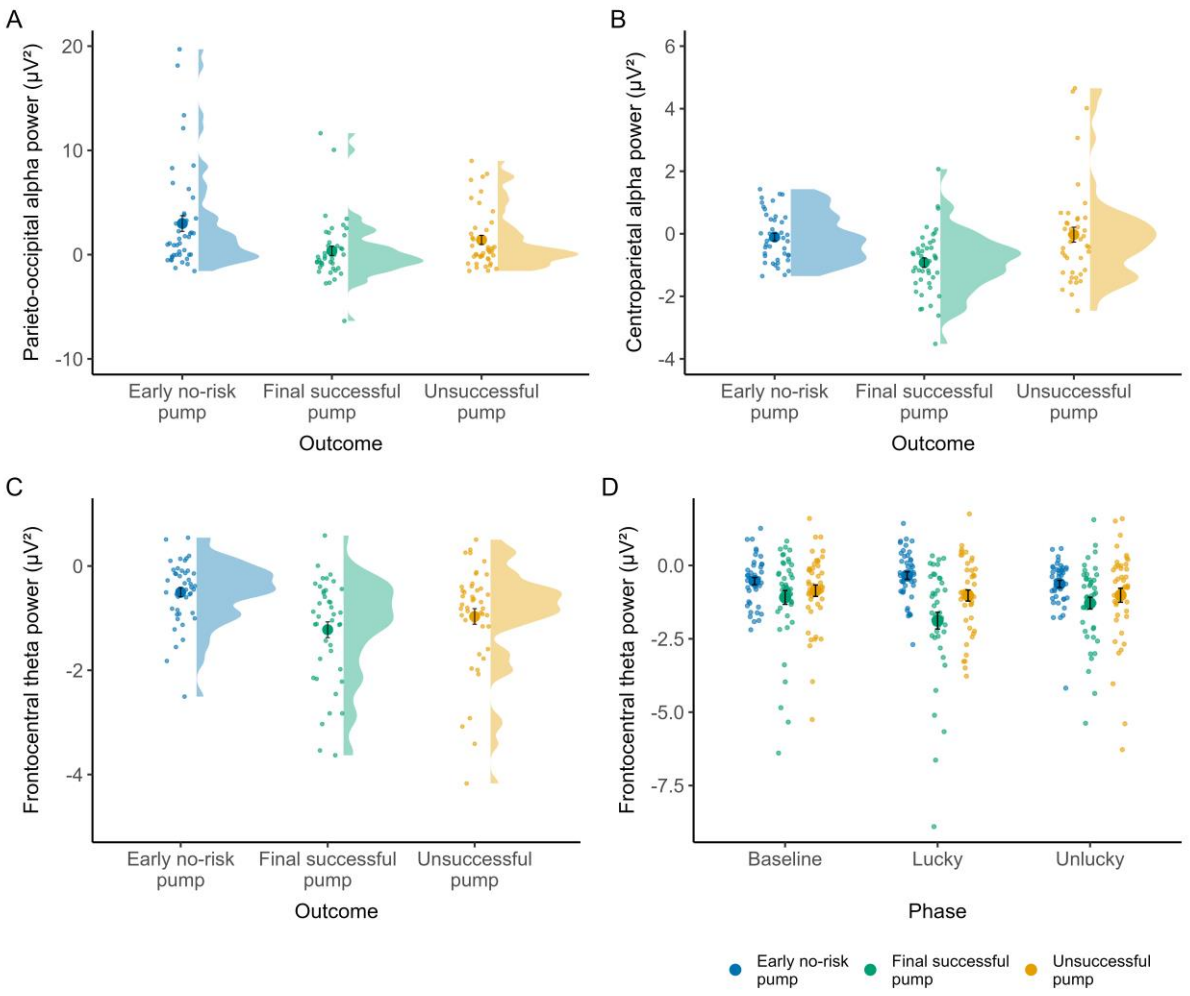

Figure 2. Induced oscillatory power across outcome types and task phases. (A) Parieto-occipital alpha power split by outcome type, with the greatest alpha power increase after early no-risk pumps. **(B)** Centroparietal alpha power split by outcome type (early no-risk pump, final successful pump, unsuccessful pump), showing the strongest alpha suppression following final successful pumps. **(C)** Frontocentral theta power split by outcome types, demonstrating a graded pattern of theta suppression, most pronounced after final successful pumps. **(D)** Frontocentral theta power split by outcome type across the three task phases (baseline, lucky, unlucky), indicating that outcome-related differences in theta suppression were most prominent during the lucky phase. Each panel displays individual data points as smaller circles (jittered to prevent overlap), group-level means as larger circles, and half-violin plots representing the distribution of power values. Note that power values are displayed in a limited range in panel A, B, and C to facilitate transparency and comparability. The values are displayed between -10 and 20 µV², until 6 µV², and over -5 µV² for subplots A, B, and C, respectively. Consequently, these subplots do not display some of those individual data points that are otherwise included in the statistical analyses (three, one, and two data points for each subplot). Error bars represent ±1 standard error of the mean (SEM).

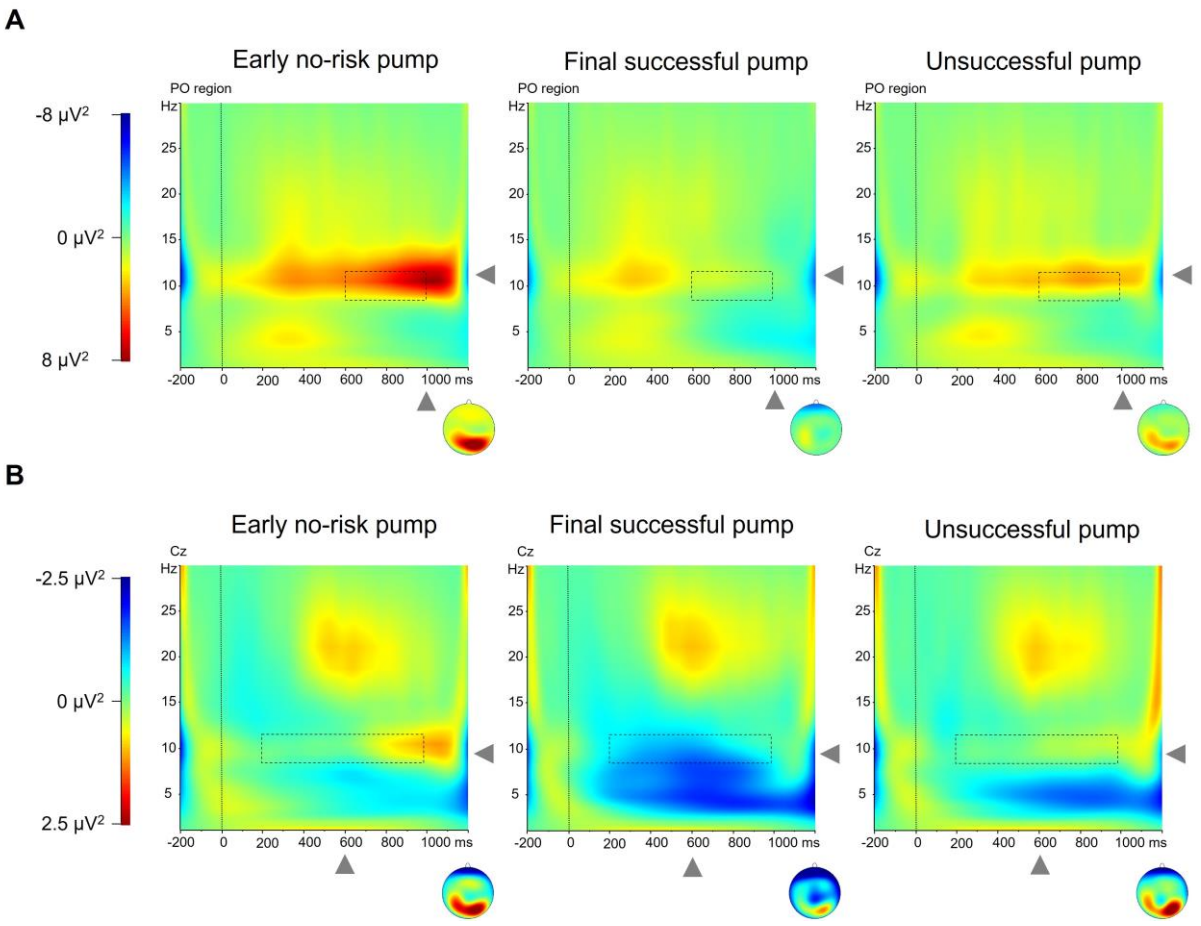

Figure 3. Time–frequency representations of induced alpha power across outcomes. (A) Grand-average time–frequency plots of alpha power over the parieto-occipital (PO) region (O1, O2, Oz, POz) across the three outcome types. The time–frequency window used for analysis (600–1000 ms post-response, 8.26 Hz to 11.74 Hz) is shown with dashed rectangles. A prominent increase in alpha power was observed after the early no-risk pumps. **(B)** Grand-average time–frequency plots of alpha power at Cz across the three outcome types. The time–frequency window used for analysis (200–1000 ms post-response, 8.26 Hz to 11.74 Hz) is shown with dashed rectangles. A prominent decrease in alpha power was observed after the final successful pumps. Topographical maps to the right of each plot illustrate the scalp distribution of alpha power at the corresponding time–frequency point (indicated by the grey arrowheads). The response (pump) onset was at 0 ms.

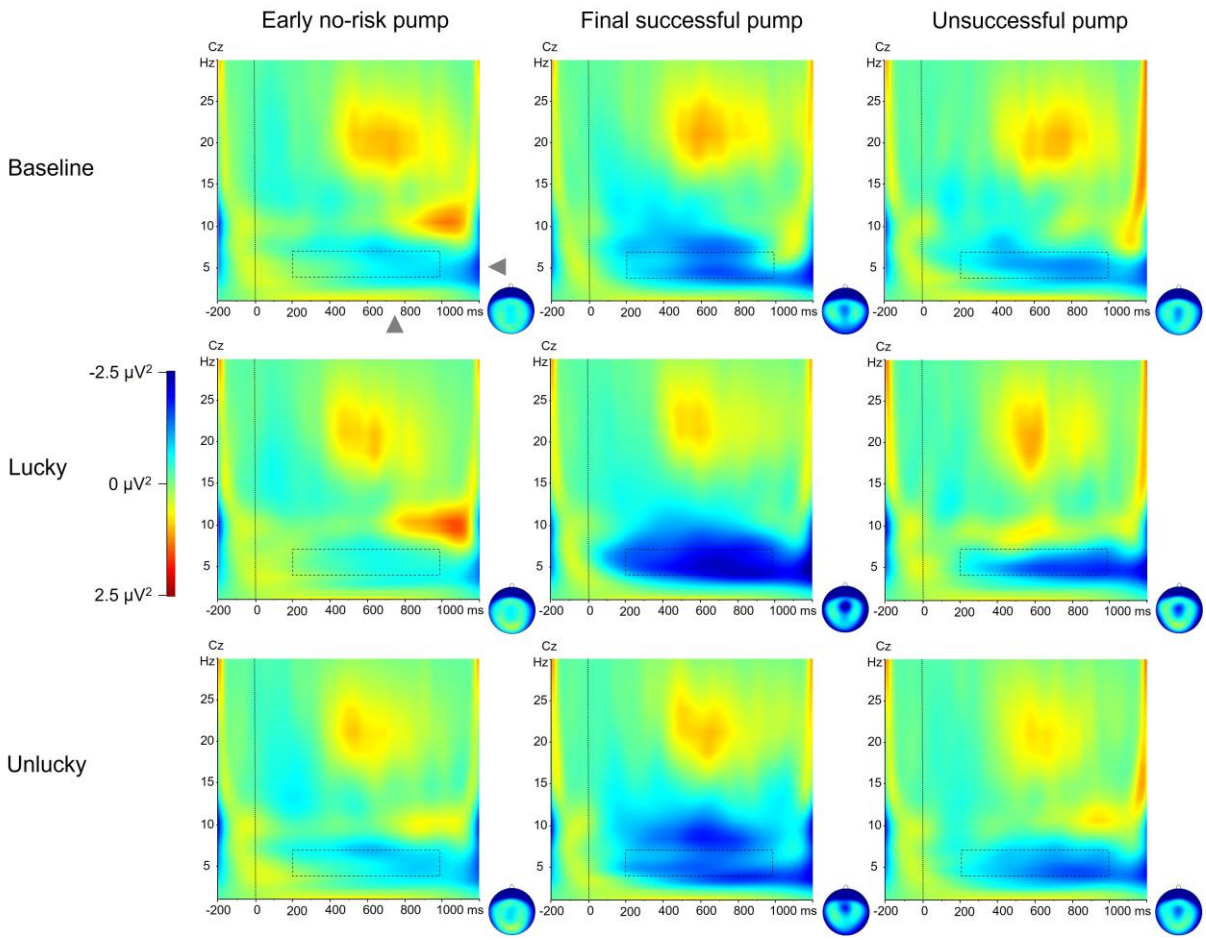

Figure 4. Time–frequency representations of induced theta power across task phases and outcomes. Grand-average time–frequency plots of theta power at Cz are displayed for each combination of task phase (baseline, lucky, unlucky) and outcome (early no-risk pump, final successful pump, unsuccessful pump). The time–frequency window used for analysis (200–1000 ms post-response, 4.09 Hz to 7.34 Hz) is shown with dashed rectangles. Theta power decreased most markedly after the final successful pumps, especially during the lucky phase. Topographical maps to the right of each plot illustrate the scalp distribution of theta power at the corresponding time–frequency point (indicated by the grey arrowheads). The response (pump) onset was at 0 ms.

Discussion

The present study investigated the neurocognitive mechanisms underlying reward anticipation during sequential decision making. To this end, induced EEG oscillatory power was measured time-locked to the critical responses of the decision-making process implemented in a modified BART. In this risky decision environment, reward probability changed over the task in a predetermined manner, but this uncertainty was unknown to participants. In terms of the EEG results, two distinct patterns emerged in the alpha frequency range. Right before the reward (inflated balloon), the parieto-occipital alpha power was increased at the early no-risk inflation

step compared to both final successful and unsuccessful inflations steps. Meanwhile, alpha power was suppressed over the centroparietal electrode sites for a more extended time after the final successful balloon inflation. This centroparietal alpha suppression was mostly lacking after the unsuccessful balloon inflation and the early no-risk inflation step. Furthermore, frontocentral theta power showed a surprising pattern, with the strongest decrease occurring after the final successful balloon inflation in the least uncertain, lucky phase. These results imply that EEG spectral components are sensitive to reward expectation and to unknown but increasing risk levels, even in the absence of explicit predictive cues.

The uncertainty manipulation played a relatively minor role at the EEG level, with risk exerting a more pronounced influence on anticipatory neural activity. This aligns with the idea that neurocognitive processes adapt rapidly to the underlying reward structure, allowing participants to adjust their expectations dynamically (Bonini et al., 2018; Kardos et al., 2016; Kóbor et al., 2021; Kóbor et al., 2023; Koscielniak et al., 2016; Petropoulos Petalas et al., 2020; Smith et al., 2016; Young & McCoy, 2019). While uncertainty effects were evident in behavioral adjustments (cf. Bán et al., 2024), the EEG findings suggest that once participants internalized the probabilistic outcome contingencies, their neural activity was primarily driven by immediate risk-reward trade-offs (moment-to-moment probability of loss) rather than broader uncertainty considerations (variability in probability estimates). This is in line with studies showing that the brain prioritizes known risk over abstract uncertainty when making real-time decisions (Tobler, O'Doherty, Dolan, & Schultz, 2007). The behavioral indices reported here (classical in the BART literature) may have been sensitive to the uncertainty manipulation due to the restricted range of possible balloon inflations in each phase of the task (see Methods). Nonetheless, these behavioral effects as well as the verbal reports indicate that decision strategies were influenced by uncertainty, potentially through neurocognitive mechanisms that were not captured by time-frequency analysis.

Studies investigating the spectral correlates of cognitive mechanism have found that alpha power increases when cognitive effort is reduced and decreases when attention and task engagement are intensified. This phenomenon is thought to reflect functional inhibition and cortical activation, respectively (e.g., Bastiaansen & Brunia, 2001; Glazer et al., 2018; Klimesch, 2012). In line with this view and our hypothesis, the increase in parieto-occipital alpha power at the early no-risk inflation step before presenting a sure reward suggests a disengagement from active anticipation. This synchronized alpha band rhythm can be considered as the operation of a "resting" or "idling" cognitive state (Pfurtscheller, Stancák, & Neuper, 1996). At this early no-risk step, effortlessly inflating the balloon further while maintaining a steady cognitive state was critical instead of expecting a certain outcome. Thus, weighing the odds of a balloon burst should have been inhibited to proceed with the task to accumulate higher earnings. Despite the absence of explicit information regarding the zero probability of the balloon bursting after the initial two pumps, it is reasonable to assume that the participants deduced this information quickly upon completing some balloons. This assumption is further substantiated by the ecological implausibility of a very early burst, given the inherent features of real balloons. Importantly, this increase in alpha power diminished or was virtually absent after the unsuccessful or final successful inflation steps, respectively. The latter finding suggests that neurocognitive mechanisms different from "idling" were engaged at the late stage of the sequential decision-making process, which we discuss next.

While we found parieto-occipital alpha increase at the early no-risk inflation step, centroparietal alpha suppression emerged after the final successful balloon inflation, most probably reflecting anticipatory attention to the forthcoming (positive) feedback (Glazer et al., 2018; Pornpattananangkul & Nusslock, 2016; van den Berg et al., 2014). At this high-risk inflation step, participants might have prepared for behavioral adjustment to cash out and collect the accumulated earnings, despite being unaware of the actual outcome of their pump

(Helfinstein et al., 2014). Meanwhile unsuccessful pumps did not show alpha suppression but a slight parieto-occipital alpha increase, which might indicate that participants were planning to continue with pumping to gain further reward, similarly to the early no-risk inflation step. The separation of successful and unsuccessful pumps based on alpha suppression might suggest that substantially different outcomes are predicted at the end of these balloon trials (Helfinstein et al., 2014; Kardos et al., 2016). Furthermore, the absence of centroparietal alpha suppression also at the early no-risk inflation step implies that attentional and expectancy processes were minimally engaged when participants did not need to anticipate potential rewards or losses.

The centroparietal distribution of the alpha suppression is contrary to our hypotheses and earlier studies, where the decrease in alpha power was found mostly over the occipital and parieto-occipital sites (Bastiaansen et al., 2002; Bastiaansen & Brunia, 2001; Gómez et al., 2004; Pornpattananangkul & Nusslock, 2016; van den Berg et al., 2014; Zhang et al., 2023). However, in the study of van den Berg et al. (2014), not only occipital alpha but also frontocentral alpha differentiated reward-prospect and no-reward-prospect trials of a cognitive conflict task, considered as the marker of increased preparatory attention to suppress irrelevant information. We speculate that the frequency range most of the alpha suppression observed in this study may be more analogous to the lower alpha range (6-10 Hz) that has been previously documented in a wide variety of paradigms (Gómez et al., 2004). This lower alpha activity is distributed in a topographically more widespread manner, extends to the anterior regions, and is likely associated with expectancy and attentional processes (Klimesch, 1999; Klimesch, Pfurtscheller, Mohl, & Schimke, 1990). Our analyses were not conducted with a focus on differentiating between lower and higher frequency ranges of alpha. Nevertheless, the centroparietal alpha suppression that occurred after the final successful balloon inflation may be indicative of a combination of increased attentional engagement and reward expectation.

Surprisingly, after successful balloon inflations, not only alpha suppression but also frontocentral theta decrease was found. This theta decrease contradicts our original hypothesis. We predicted decreased theta at the early no-risk inflation step relative to the final inflation steps due to the more probable reward (Bunzeck et al., 2011; Doñamayor et al., 2012). However, the present results suggest the opposite, i.e., expecting more probable rewards at the end of the balloon inflation process, especially in the case of balloon inflations that resulted in an actual reward. It is conceivable that expectations regarding the success of the current pump may have become relatively optimistic or marginally positively biased over the balloon inflation process. Participants may have anticipated a reward instead of a balloon burst, implicitly recognizing the success of their pump even before receiving the actual feedback. However, in the case of unsuccessful pumps, expectations could have been ambiguous with the intention to continue the balloon inflation, as evidenced by the less pronounced theta and alpha decrease and a small degree of alpha increase.

This interpretation does not fully align with the findings of previous studies showing that theta increases before potential rewards (Alí Diez et al., 2024; Reinhart & Woodman, 2014; Zhang et al., 2023). The discrepancy could arise from the sequential nature of the BART, where expectancy evolves dynamically rather than reward probability being explicitly signaled by a cue. Therefore, the observed theta decrease might reflect a learned adaptation to the reward structure. It is also possible that the characteristics of theta oscillations shift in self-paced decision-making contexts, such as the present one, compared to externally cued ones. However, it should be noted that substantially more results are available about the modulations of theta oscillation related to the reward-outcome stage (Glazer et al., 2018). Consequently, further research is necessary to determine how the theta oscillations indeed change during reward anticipation and what could be their general functional significance.

It is noteworthy that the theta decrease and its difference between the risk levels were most pronounced in the lucky phase, where burst probability was reduced. This is contrary to our initial hypotheses, as we predicted reward probability effects would be largest in the most uncertain unlucky phase. Due to the flatter burst probability function in the lucky phase, a sequence of successful pumps had the potential to yield a larger reward. Considering the actual behavioral results on the points collected, a greater amount of reward could be lost in the lucky phase than in the unlucky phase. Therefore, participants might have dedicated special attention and incentive value to the balloons presented in the lucky phase. Collectively, the results on theta decrease, in conjunction with the parieto-occipital alpha increase linked mostly to the early no-risk step and, may suggest that distinct neurocognitive mechanisms are engaged at the different stages of the sequential decision-making process. Namely, theta decrease appears to be particularly sensitive to the unknown probability of proximal rewards actually occurring at the end of the balloon inflation process. This sensitivity is not evident after the early no-risk pump, where the absolute certainty of reward, or at least the step-by-step accumulation of a future reward, is more significant.

Despite the absence of explicit cues signaling reward probability at each pump, the visual presentation of the current balloon throughout the anticipatory period likely served as an implicit reward-predicting cue. The balloon's size and prior inflation history carried information about the potential risk of a balloon burst, based on which participants might have developed implicit reward expectations. In fact, the analysis revealed that centroparietal alpha and frontocentral theta activity differentiated actions similar at the surface level – final balloon inflations – based on their forthcoming, but as yet unknown, success, even before the outcome was revealed. This supports the idea that expectations regarding the probabilistic reward structure, implicitly learned through repeated experiences, plays a pivotal role during reward

anticipation in uncertain decision environments (Bonini et al., 2018; Helfinstein et al., 2014; Kardos et al., 2016; Koscielniak et al., 2016; Petropoulos Petalas et al., 2020).

Although modulations of beta oscillations have often been linked to reward anticipation and motor preparation (Apitz & Bunzeck, 2014; Bunzeck et al., 2011; Reinhart & Woodman, 2014; Xiao et al., 2024), these were absent in the present study. This might imply that modulations of beta activity could be more prominent in tasks with explicit reward cues, however, more research is needed to clarify their specific role in paradigms such as the BART. Though, in our data, indications were found for the presence of increased beta activity over the anterior-central electrode sites (see Figures 3-4). However, this increased beta activity appeared similarly across phases and risk levels. Therefore, we speculate that beta activity in this experiment may not be directly associated with reward anticipation; rather, it may be implicated in the maintenance of the current sensorimotor and cognitive sets while waiting for the outcome to occur (Engel & Fries, 2010). A change in the motor response happens when the participant decides to cash out and collect the accumulated earnings. Nevertheless, this action does not seem to be as unambiguous and deliberate as would be signaled by a genuine increase in beta activity merely prior to the presentation of the final inflated balloon (Jenkinson & Brown, 2011). In accordance with this line of reasoning, we have already interpreted the decreased theta activity as reflecting positively biased reward anticipation after the final inflation step, where the cash-out response may have remained undecided. Recent research has suggested that increased beta activity may serve as a neurophysiological marker of implicit statistical learning (Bogaerts, Richter, Landau, & Frost, 2020). Nonetheless, the implications of this finding for implicitly learned reward regularities, such as those in the BART, are yet to be elucidated.

While our results advance the understanding of reward anticipation in sequential decision making, some methodological limitations should be considered. Focusing only on the anticipation phase in a response-locked manner allowed us to capture neurocognitive responses

that were relatively comparable across phases and inflation steps. In this task version, analyzing the outcome stage in a stimulus-locked manner involves comparing either different visual stimuli for reward (inflated balloon or cash-out screen) and non-reward (balloon burst) trials (Kóbor et al., 2015) or various reward magnitudes (balloon sizes) if only the successfully inflated balloons are considered (Kardos et al., 2016). Even in the present study, the short duration of the anticipatory window, the challenge of establishing an EEG segment baseline without stimulus presentation and response preparation, and the potentially confounding balloon size as a reward cue should be considered in interpreting these results. For instance, the short anticipatory window did not allow us to reliably measure delta oscillations that have been found to be modulated mostly in the cue-evaluation substage of reward anticipation (Glazer et al., 2018).

Most of these limitations are related to the characteristics of the paradigm and were considered necessary to create an ecologically valid task that mimics everyday risk raking. Despite these limitations, our findings provide a novel contribution to the understanding of reward anticipation: They demonstrate that spectral components differentiate between risk levels and outcome expectations even in the absence of explicit cues. Together, the findings underscore the simultaneous operation of at least two processes, wherein participants maintain a consistent cognitive state, and an expectation-driven process that modulates alpha and theta dynamics in response to evolving risk and reward probabilities. Future research should delve deeper into the functional significance of theta and alpha modulations in implicit reward prediction and adaptive decision making.

Declarations

Ethics approval and consent to participate

The study was conducted in accordance with the Declaration of Helsinki. The United Ethical Review Committee for Research in Psychology (EPKEB) in Hungary gave approval to the procedure. Written informed consent was obtained from all participants.

Consent for publication

Not applicable.

Data availability statement

Data supporting the findings of this study (processed behavioral and time-frequency data) are available via the Open Science Framework (https://osf.io/bwzfa/files/osfstorage), located in the BART luck FC TF folder. EEG data in various formats (raw, pre-processed, segmented, etc.) will be provided from the corresponding author (A.K.) upon written request. The experiment was not preregistered.

Code availability statement

Not applicable as no custom code was used to process the data described in the study.

Competing interests

The authors declare no competing interests.

Funding information

This research was supported by project no. 124412 (PI: A.K.) that have been implemented with the support provided by the Ministry of Innovation and Technology of Hungary from the

National Research, Development and Innovation Fund, financed under the FK funding scheme. Furthermore, the research was supported by the National Brain Research Program by the Hungarian Academy of Sciences (project NAP2022-I-1/2022) and the János Bolyai Research Scholarship of the Hungarian Academy of Sciences.

Acknowledgements

The authors thank Noémi Éltető and Zsófia Kardos for their helpful suggestions on the experimental design. They also thank the help of Dóra Bárány in EEG data acquisition, and the useful comments of Dezső Nemeth and Ferenc Honbolygó on the earlier version of the manuscript.

CRediT author statement

Eszter Tóth-Fáber: Conceptualization, Methodology, Project administration, Investigation, Formal analysis, Data Curation, Writing – Original Draft, Writing – Review & Editing, Visualization.

Andrea Kóbor: Conceptualization, Methodology, Software, Project administration, Formal analysis, Data Curation, Supervision, Funding acquisition, Writing – Original Draft, Writing – Review & Editing.

Use of AI Generated Content (AIGC) and tools

During the preparation of this work the authors used ChatGPT-4 and DeepL to improve the writing style. After using this tool/service, the authors reviewed and edited the content as needed and took full responsibility for the content of the publication.

References

Alí Diez, I., Fàbrega-Camps, G., Parra-Tíjaro, J., & Marco-Pallarés, J. (2024). Anticipatory and consummatory neural correlates of monetary and music rewarding stimuli. *Brain and Cognition, 179*, 106186. doi:10.1016/j.bandc.2024.106186

Apitz, T., & Bunzeck, N. (2014). Early Effects of Reward Anticipation Are Modulated by Dopaminergic Stimulation. *PLoS ONE, 9*(10), e108886. doi:10.1371/journal.pone.0108886

Bán, K., Tóth-Fáber, E., Lages, M., & Kóbor, A. (2024, October 01, 2024). *Uncertainty-dependent learning bias in value-based decision making*. OSF Preprints.

Bastiaansen, M. C. M., Böcker, K. B. E., & Brunia, C. H. M. (2002). ERD as an index of anticipatory attention? Effects of stimulus degradation. *Psychophysiology, 39*(1), 16-28. doi:10.1017/S0048577202000483

Bastiaansen, M. C. M., & Brunia, C. H. M. (2001). Anticipatory attention: an event-related desynchronization approach. *International Journal of Psychophysiology, 43*(1), 91-107. doi:10.1016/S0167-8760(01)00181-7

Bastiaansen, M. C. M., Mazaheri, A., & Jensen, O. (2012). Beyond ERPs: Oscillatory neuronal dynamics. In *The Oxford handbook of event-related potential components.* (pp. 31-49). New York, NY, US: Oxford University Press.

Berridge, K. C., & Robinson, T. E. (2003). Parsing reward. *Trends in Neurosciences, 26*(9), 507-513. doi:10.1016/S0166-2236(03)00233-9

Berridge, K. C., Robinson, T. E., & Aldridge, J. W. (2009). Dissecting components of reward: ‘liking’, ‘wanting’, and learning. *Current Opinion in Pharmacology, 9*(1), 65-73. doi:10.1016/j.coph.2008.12.014

Bogaerts, L., Richter, C. G., Landau, A. N., & Frost, R. (2020). Beta-Band Activity Is a Signature of Statistical Learning. *The Journal of Neuroscience, 40*(39), 7523. doi:10.1523/JNEUROSCI.0771-20.2020

Bonini, N., Grecucci, A., Nicolè, M., & Savadori, L. (2018). Reduced Risk-Taking After Prior Losses in Pathological Gamblers Under Treatment and Healthy Control Group but not in Problem Gamblers. *Journal of Gambling Studies, 34*(2), 429-447. doi:10.1007/s10899-017-9709-z

Bunzeck, N., Guitart-Masip, M., Dolan, R. J., & Düzel, E. (2011). Contextual Novelty Modulates the Neural Dynamics of Reward Anticipation. *The Journal of Neuroscience, 31*(36), 12816. doi:10.1523/JNEUROSCI.0461-11.2011

Cohen, M. X. (2014). *Analyzing neural time series data: theory and practice*: MIT press.

De Groot, K. (2020). Burst Beliefs – Methodological Problems in the Balloon Analogue Risk Task and Implications for Its Use. *Journal of Trial and Error, 1*(1). doi:10.36850/mr1

De Groot, K., & Thurik, R. (2018). Disentangling Risk and Uncertainty: When Risk-Taking Measures Are Not About Risk. *Frontiers in Psychology, 9*(2194). doi:10.3389/fpsyg.2018.02194

Delorme, A., Sejnowski, T., & Makeig, S. (2007). Enhanced detection of artifacts in EEG data using higher-order statistics and independent component analysis. *Neuroimage, 34*(4), 1443-1449. doi:10.1016/j.neuroimage.2006.11.004

Doñamayor, N., Schoenfeld, M. A., & Münte, T. F. (2012). Magneto- and electroencephalographic manifestations of reward anticipation and delivery. *Neuroimage, 62*(1), 17-29. doi:10.1016/j.neuroimage.2012.04.038

Dragovic, M. (2004a). Categorization and validation of handedness using latent class analysis. *Acta Neuropsychiatrica, 16*(4), 212-218. doi:10.1111/j.0924-2708.2004.00087.x

Dragovic, M. (2004b). Towards an improved measure of the Edinburgh Handedness Inventory: a one-factor congeneric measurement model using confirmatory factor analysis. *Laterality: Asymmetries of Body, Brain and Cognition, 9*(4), 411-419. doi:10.1080/13576500342000248

Edgar, E. V., Waugh, A., Wu, J., Castagna, P., Potenza, M. N., Mayes, L. C., & Crowley, M. J. (2024). Risk avoidance and social anxiety in adolescence: Examination of event-related potentials and theta-dynamics on the Balloon Risk Avoidance Task. *Brain and Cognition, 180*, 106209. doi:10.1016/j.bandc.2024.106209

Engel, A. K., & Fries, P. (2010). Beta-band oscillations—signalling the status quo? *Current Opinion in Neurobiology, 20*(2), 156-165. doi:10.1016/j.conb.2010.02.015

Fein, G., & Chang, M. (2008). Smaller feedback ERN amplitudes during the BART are associated with a greater family history density of alcohol problems in treatment-naive alcoholics. *Drug and Alcohol Dependence, 92*(1-3), 141-148. doi:10.1016/j.drugalcdep.2007.07.017

Fryer, S. L., Roach, B. J., Holroyd, C. B., Paulus, M. P., Sargent, K., Boos, A., . . . Mathalon, D. H. (2021). Electrophysiological investigation of reward anticipation and outcome evaluation during slot machine play. *Neuroimage, 232*, 117874. doi:10.1016/j.neuroimage.2021.117874

Glazer, J. E., Kelley, N. J., Pornpattananangkul, N., Mittal, V. A., & Nusslock, R. (2018). Beyond the FRN: Broadening the time-course of EEG and ERP components implicated in reward processing. *International Journal of Psychophysiology, 132*, 184-202. doi:10.1016/j.ijpsycho.2018.02.002

Gómez, C. M., Vaquero, E., López-Mendoza, D., González-Rosa, J., & Vázquez-Marrufo, M. (2004). Reduction of EEG power during expectancy periods in humans. *Acta Neurobiol Exp (Wars), 64*(2), 143-151. doi:10.55782/ane-2004-1500

Greenhouse, S., & Geisser, S. (1959). On methods in the analysis of profile data. *Psychometrika, 24*(2), 95-112. doi:10.1007/bf02289823

Gu, R., Zhang, D., Luo, Y., Wang, H., & Broster, L. S. (2018). Predicting risk decisions in a modified Balloon Analogue Risk Task: Conventional and single-trial ERP analyses. *Cognitive, Affective, & Behavioral Neuroscience, 18*(1), 99-116. doi:10.3758/s13415-017-0555-3

Helfinstein, S. M., Schonberg, T., Congdon, E., Karlsgodt, K. H., Mumford, J. A., Sabb, F. W., . . . Poldrack, R. A. (2014). Predicting risky choices from brain activity patterns. *Proceedings of the National Academy of Sciences, 111*(7), 2470-2475. doi:10.1073/pnas.1321728111

Hertwig, R., & Erev, I. (2009). The description-experience gap in risky choice. *Trends in Cognitive Sciences, 13*(12), 517-523. doi:10.1016/j.tics.2009.09.004

Jenkinson, N., & Brown, P. (2011). New insights into the relationship between dopamine, beta oscillations and motor function. *Trends in Neurosciences, 34*(12), 611-618. doi:10.1016/j.tins.2011.09.003

Kardos, Z., Kóbor, A., Takács, A., Tóth, B., Boha, R., File, B., & Molnár, M. (2016). Age-related characteristics of risky decision-making and progressive expectation formation. *Behavioural Brain Research, 312*, 405-414. doi:10.1016/j.bbr.2016.07.003

Kiat, J., Straley, E., & Cheadle, J. E. (2016). Escalating risk and the moderating effect of resistance to peer influence on the P200 and feedback-related negativity. *Social Cognitive and Affective Neuroscience, 11*(3), 377-386. doi:10.1093/scan/nsv121

Klimesch, W. (1999). EEG alpha and theta oscillations reflect cognitive and memory performance: a review and analysis. *Brain Research Reviews, 29*(2), 169-195. doi:10.1016/S0165-0173(98)00056-3

Klimesch, W. (2012). Alpha-band oscillations, attention, and controlled access to stored information. *Trends in Cognitive Sciences, 16*(12), 606-617. doi:10.1016/j.tics.2012.10.007

Klimesch, W., Pfurtscheller, G., Mohl, W., & Schimke, H. (1990). Event-related desynchronization, ERD-mapping and hemispheric differences for words and numbers. *International Journal of Psychophysiology, 8*(3), 297-308. doi:10.1016/0167-8760(90)90020-E

Knight, F. H. (1921). *Risk, uncertainty and profit*. New York, NY: Sentry Press.

Kóbor, A., Kardos, Z., Takács, Á., Éltető, N., Janacsek, K., Tóth-Fáber, E., . . . Nemeth, D. (2021). Adaptation to recent outcomes attenuates the lasting effect of initial experience on risky decisions. *Scientific Reports, 11*(1), 10132. doi:10.1038/s41598-021-89456-1

Kóbor, A., Takács, A., Janacsek, K., Németh, D., Honbolygó, F., & Csépe, V. (2015). Different strategies underlying uncertain decision making: Higher executive performance is associated with enhanced feedback-related negativity. *Psychophysiology, 52*(3), 367-377. doi:10.1111/psyp.12331

Kóbor, A., Tóth-Fáber, E., Kardos, Z., Takács, Á., Éltető, N., Janacsek, K., . . . Nemeth, D. (2023). Deterministic and probabilistic regularities underlying risky choices are acquired in a changing decision context. *Scientific Reports, 13*(1), 1127. doi:10.1038/s41598-023-27642-z

Koscielniak, M., Rydzewska, K., & Sedek, G. (2016). Effects of Age and Initial Risk Perception on Balloon Analog Risk Task: The Mediating Role of Processing Speed and Need for Cognitive Closure. *Frontiers in Psychology, 7*(659). doi:10.3389/fpsyg.2016.00659

Lejuez, C. W., Read, J. P., Kahler, C. W., Richards, J. B., Ramsey, S. E., Stuart, G. L., . . . Brown, R. A. (2002). Evaluation of a behavioral measure of risk taking: the Balloon

Analogue Risk Task (BART). *Journal of Experimental Psychology: Applied, 8*(2), 75-84. doi:10.1037//1076-898X.8.2.75

Li, P., Baker, T. E., Warren, C., & Li, H. (2016). Oscillatory profiles of positive, negative and neutral feedback stimuli during adaptive decision making. *International Journal of Psychophysiology, 107*, 37-43. doi:10.1016/j.ijpsycho.2016.06.018

Lopez-Gamundi, P., Mas-Herrero, E., & Marco-Pallares, J. (2024). Disentangling effort from probability of success: Temporal dynamics of frontal midline theta in effort-based reward processing. *Cortex, 176*, 94-112. doi:10.1016/j.cortex.2024.03.014

Makeig, S., Westerfield, M., Jung, T.-P., Enghoff, S., Townsend, J., Courchesne, E., & Sejnowski, T. J. (2002). Dynamic Brain Sources of Visual Evoked Responses. *Science, 295*(5555), 690-694. doi:doi:10.1126/science.1066168

Meyer, G. M., Marco-Pallarés, J., Boulinguez, P., & Sescousse, G. (2021). Electrophysiological underpinnings of reward processing: Are we exploiting the full potential of EEG? *Neuroimage, 242*, 118478. doi:10.1016/j.neuroimage.2021.118478

Oldfield, R. C. (1971). The assessment and analysis of handedness: The Edinburgh inventory. *Neuropsychologia, 9*(1), 97-113. doi:10.1016/0028-3932(71)90067-4

Petropoulos Petalas, D., Bos, S., Hendriks Vettehen, P., & van Schie, H. T. (2020). Event-related brain potentials reflect predictive coding of anticipated economic change. *Cognitive, Affective, & Behavioral Neuroscience, 20*(5), 961-982. doi:10.3758/s13415-020-00813-5

Pfurtscheller, G., Stancák, A., & Neuper, C. (1996). Event-related synchronization (ERS) in the alpha band - an electrophysiological correlate of cortical idling: A review. *International Journal of Psychophysiology, 24*(1-2), 39-46. doi:10.1016/S0167-8760(96)00066-9

Pornpattananangkul, N., & Nusslock, R. (2016). Willing to wait: Elevated reward-processing EEG activity associated with a greater preference for larger-but-delayed rewards. *Neuropsychologia, 91*, 141-162. doi:10.1016/j.neuropsychologia.2016.07.037

Qianlan, Y., Shou, C., Tianya, H., Wei, D., & Liu, T. (2025). Sensation seeking and risk adjustment: the role of reward sensitivity in dynamic risky decisions. *Frontiers in Behavioral Neuroscience, 19*. doi:10.3389/fnbeh.2025.1492312

Reinhart, R. M., & Woodman, G. F. (2014). Oscillatory coupling reveals the dynamic reorganization of large-scale neural networks as cognitive demands change. *Journal of Cognitive Neuroscience, 26*(1), 175-188. doi:10.1162/jocn_a_00470

Schmitz, F., Manske, K., Preckel, F., & Wilhelm, O. (2016). The Multiple Faces of Risk-Taking. *European Journal of Psychological Assessment, 32*(1), 17-38. doi:10.1027/1015-5759/a000335

Schonberg, T., Fox, C. R., & Poldrack, R. A. (2011). Mind the gap: bridging economic and naturalistic risk-taking with cognitive neuroscience. *Trends in Cognitive Sciences, 15*(1), 11-19. doi:10.1016/j.tics.2010.10.002

Smith, A. R., Ebert, E. E., & Broman-Fulks, J. J. (2016). The relationship between anxiety and risk taking is moderated by ambiguity. *Personality and Individual Differences, 95*, 40-44. doi:10.1016/j.paid.2016.02.018

Tallon-Baudry, C., & Bertrand, O. (1999). Oscillatory gamma activity in humans and its role in object representation. *Trends in Cognitive Sciences, 3*(4), 151-162. doi:10.1016/S1364-6613(99)01299-1

Tao, R., Zhang, C., Zhao, H., Xu, Y., Han, T., Dai, M., . . . Xu, S. (2023). A negative emotional context disrupts the framing effect on outcome evaluation in decision making under uncertainty: An ERP study. *Psychophysiology, 60*(4), e14207. doi:10.1111/psyp.14207

Tobler, P. N., O'Doherty, J. P., Dolan, R. J., & Schultz, W. (2007). Reward Value Coding Distinct From Risk Attitude-Related Uncertainty Coding in Human Reward Systems. *Journal of Neurophysiology, 97*(2), 1621-1632. doi:10.1152/jn.00745.2006

van den Berg, B., Krebs, R. M., Lorist, M. M., & Woldorff, M. G. (2014). Utilization of reward-prospect enhances preparatory attention and reduces stimulus conflict. *Cognitive, Affective, & Behavioral Neuroscience, 14*(2), 561-577. doi:10.3758/s13415-014-0281-z

Xiao, J., Adkinson, J. A., Myers, J., Allawala, A. B., Mathura, R. K., Pirtle, V., . . . Sheth, S. A. (2024). Beta activity in human anterior cingulate cortex mediates reward biases. *Nature Communications, 15*(1), 5528. doi:10.1038/s41467-024-49600-7

Xu, S. (2021). Self–other discrepancies in electrophysiological response to outcome evaluation in the Balloon Analogue Risk Task. *International Journal of Psychophysiology, 170*, 6-11. doi:10.1016/j.ijpsycho.2021.09.010

Young, M. E., & McCoy, A. W. (2019). Variations on the balloon analogue risk task: A censored regression analysis. *Behavior Research Methods, 51*(6), 2509-2521. doi:10.3758/s13428-018-1094-8

Zhang, Y., Li, Q., Rong, Y., Hu, L., Müller, H. J., & Wei, P. (2023). Comparing monetary gain and loss in the monetary incentive delay task: EEG evidence. *60*(12), e14383. doi:10.1111/psyp.14383